Experimental and Computational Studies of MHD Relaxation Generated by Coaxial Helicity Injection in the HIST Spherical Torus Plasmas

M. Nagata 1), Y. Kikuchi 1), T. Kanki 2), N. Fukumoto 1), Y. Kagei 3)

1) Univerisity of Hyogo, Himeji, Hyogo 671-2201, Japan
2) Japan Coast Guard Academy, Kure, Hiroshima 737-8512, Japan
3) Research Organization for Information Science & Technology, Tokai, Ibaraki 319-1106, Japan

e-mail contact of main author: nagata@eng.u-hyogo.ac.jp

Abstract. Coaxial Helicity Injection (CHI) experiments in the Helicity Injected Spherical Torus (HIST) device have produced discharges with peak plasma currents up to 150 kA and successfully sustained the plasma current for much longer than a resistive decay time. The flow measurements using a Mach probe have shown that the intermittent generation of the flow is correlated to the fluctuation seen on the electron density and current signals. The repetitive merging of the magnetized plasma jet ejected from the helicity injector may be responsible for the current sustainment in these discharges. This CHI current drive mechanism is supported by the 3D-MHD numerical simulation. The acceleration of ion flow up to ~50 km/s has been observed during the transition phase from the spherical torus (ST) to the flipped-ST relaxed state. We have found that the current self-reversal process involves the non-linear growth of the n=1 kink instability of the central column and the relevant magnetic reconnection flow.

1. Introduction

Non-inductive plasma startup and current drive by CHI using a magnetized coaxial plasma gun (MCPG) have been successfully demonstrated for spheromak (SPHEX [1], FACT [2], SSPX [3]) and spherical torus (ST) plasmas (HIST [4], HIT-II [5], NSTX [6],) that have a potential to lead to an attractive steady-state high-beta fusion reactor. The HIST device (R=0.30 m, a=0.24 m, A=1.25) [4] can form and sustain the normal ST (high-q: q>1 and ultra-low-q (ULQ) including spheromaks: q<1) and the flipped ST (F-ST) plasmas by utilizing the variation of the external toroidal field (TF) coil current $I_{\mathrm{tf.}}$. For the normal ST (N-ST) in the high-q operation regime, the toroidal current I_{t} generated by CHI increases up to 150 kA. The average electron density $\bar{n}_e$ is in the range of 2-9×10^{19} m^{-3} and the sustainment time is 3-5 ms. The F-ST configuration has been for the first time found in the HIST device [7]. One of main purposes is to investigate current drive mechanisms, its relevant plasma flows and MHD relaxation in the both N-ST and F-ST configurations, and to control them by using an externally applied rotating magnetic field (RMF).

An electron locking model [8] was proposed as a possible mechanism for current drive with CHI and its validity was confirmed by accounting for experimental observations in the HIT-II [8] and the NSTX devices [6]. In the NSTX, the plasma flow (~20 km/s) is driven in the $\boldsymbol{E}\times\boldsymbol{B}$ toroidal direction by CHI which has the same direction as the n=1 mode. Another possible mechanism is relied on the repetitive plasmoid injection from the MCPG and the following merging process. In the HIST device, the phenomena of coalescence of annuli coincided with the repetitive current generation were observed during the sustainment by internal magnetic probe measurements [4]. This process involves kinking behaviors of the plasma flow ejected from the MCPG. To identify these detail mechanisms, it is needed to manifest a role of flow in the dynamo current drive. Application of useful flow measurements is a key point for this study. Thus we have used Mach probes and ion Doppler spectroscopic measurements. In parallel simulation studies are needed for the comparison between theory and experiment.

Resistive, single-fluid 3D MHD numerical simulations (MHDTM-code) [9, 10] reproduce the formation and sustainment of the ULQ-ST and the F-ST and contribute to further understanding of CHI relaxation and magnetic reconnection physics.

2. Experimental set-up and flow measurements

A schematic view of the HIST device and diagnostics used in this experiment is shown in Fig. 1. Three axis magnetic probes (B_r, B_θ, B_z) are installed in the plasma at a distance of z = 0.74 m from the midplane (z = 0 m) of the spherical solid copper flux conserver (FC) (diameter: 1.0 m, thickness: 3 mm). Magnetic pick-up coils (16 channels for B_z) are located in the poloidal direction along the inner surface of the FC to calculate the total toroidal plasma current I_t. Each poloidal flux topology of the N-ST and the F-ST configurations is illustrated in the drawing of the HIST. An interesting point for the F-ST configuration is that the non-flipped region exists near the MCPG muzzle. A six channels λ probe incorporating small size Rogowski and flux loops is used to measure toroidal current density and toroidal flux profiles on the FC midplane. The toroidal n mode number of the magnetic fluctuations of B_t is measured using eight magnetic pick up coils distributed toroidally at equal angles over 360 degrees and around the outer edge. The line averaged electron density are measured by a CO_2 laser interferometer.

Ion flow measurements have been conducted by internal Mach probes. The Mach probe consists of nine tungsten rods surrounding glass-ceramic (Macor) as shown in Fig. 2. Toroidal and poloidal ion flows can be simultaneously measured. An ion flow velocity V_i is calculated by $V_i = C_s M_i$, where C_s is an ion sound velocity (~30 km/s, T_e=T_i). An ion Mach number M_i can be obtained from $M_i = M_c \ln(J_{up}/J_{down})$, where M_c is a proportionality constant that depends on T_e and T_i, and where J_{up} and J_{down} are ion current densities measured by upstream and downstream rod probes, respectively. Because the probe radius is smaller than the ion Larmor radius (>1 cm), the unmagnetized condition is satisfied in the theoretical model which determines M_c = 0.53 (assuming that T_e=T_i) in this case.

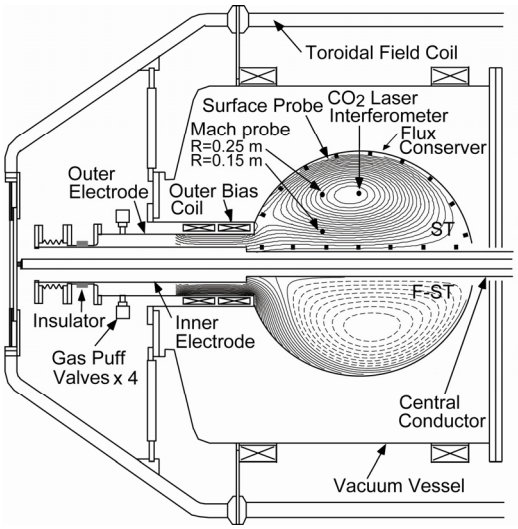

FIG.1 Schematic diagram of the HIST device and a magnetic configuration of ST and Flipped ST.

Ion Doppler Spectrometer (IDS) using a compact 16 channel photomultiplier tube (R5900U-03-L16, Hamamatsu Photonics Co.Ltd.) has been developed in order to measure ion temperature $T_{i,D}$ and ion flow velocity $v_{i,D}$. The IDS system consists of a light collection system including optical fibers, 1 m-spectrometer (resolution: 0.0085nm) and the PMT detector. Technical details of the similar IDS system are reported in reference [11]. In this experiment, the optical fiber covered with

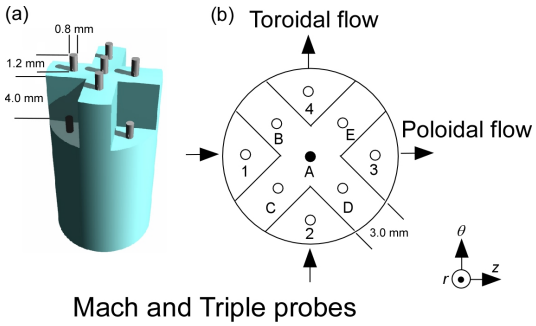

FIG.2. Schematic view of 2D Mach probe.

glass tubes is inserted into the plasma, and so the radial profile of $T_{i.D}$ and $v_{i.D}$ can be measured.

3. Plasma flow driven during CHI

Figure 3 illustrates temporal evolutions of I_t, $\bar{n}_e$ and the toroidal flow velocity $v_{i.t}$ measured using the Mach probe. The intermittent generation of I_t with a frequency of 10-20 kHz has been observed in the high-q ST discharges in which the high plasma current (I_t>50 kA) can be maintained. The fluctuations seen on the density and the ion flow are fairly correlated with the generation of the I_t. The velocity of the intermittent flow expressed by "bubble-burst" is enhanced up to $v_{i.t}$=20-40 km/s during the strongly driven phase. This flow is driven in the opposite direction of the I_t and superimposed on the $\boldsymbol{E}\times\boldsymbol{B}$ rotation induced by an applied voltage. After t=1.6 ms, the discharge tends to change to the partially driven phase mixed with a resistive decay so that the direction of the flow observed in the core region tends to reverse and results in the same as that of I_t.

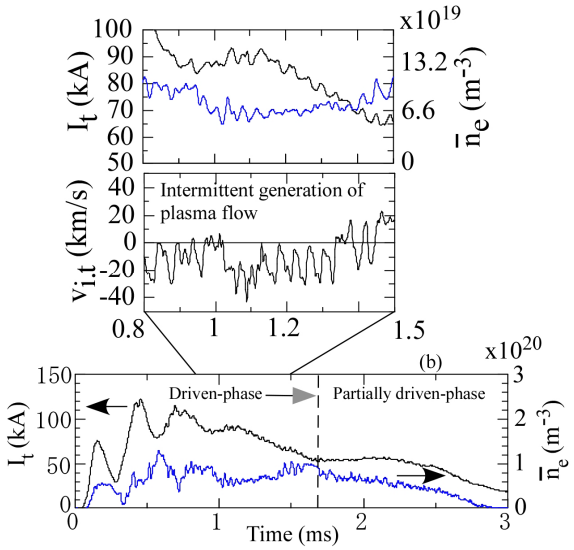

FIG.3. Time evolution of toroidal current, electron density and the toroidal flow $v_{i.t}$ measured at R=0.15 m by a Mach probe. Note that the direction of the intermittent flow is opposite to that of I_t in the driven-phase.

The toroidal ion flow is thought to be driven by the magnetic reconnection event occurring intermittently at the X-point during the merging process. This result is consistent with the model that depends on the MCPG injector-based reconnection activity requiring rotation of the magnetic field around the injector region [5]. The plasma jet emanating from the MCPG and the generation of a magnetized plasmoid by the reconnection is very well reflected in the 3D MHD simulation as described below.

4. 3D MHD simulation methods and results

Nonlinear MHD numerical simulations have been performed to identify the current drive mechanisms by CHI. Figure 4 shows a three-dimensional full-toroidal cylindrical (r, θ, z) geometry used in this simulation. The governing equations are the set of the nonlinear resistive MHD equations as follows:

$$\frac{\partial \rho \boldsymbol{v}}{\partial t} = -\nabla\cdot\rho\boldsymbol{v}\boldsymbol{v} + \boldsymbol{j}\times\boldsymbol{B} - \nabla p - \nabla\cdot\ddot{\boldsymbol{\Pi}}, \tag{1}$$

$$\frac{\partial \boldsymbol{B}}{\partial t} = -\nabla\times\boldsymbol{E}, \tag{2}$$

$$\frac{\partial p}{\partial t} = -\nabla\cdot(p\boldsymbol{v} - \kappa\nabla T) - (\gamma-1)(p\nabla\cdot\boldsymbol{v} + \ddot{\boldsymbol{\Pi}} : \nabla\boldsymbol{v} - \eta j^2), \tag{3}$$

$$\boldsymbol{E} = -\boldsymbol{v}\times\boldsymbol{B} + \eta\boldsymbol{j}, \tag{4}$$

$$\boldsymbol{j} = \nabla\times\boldsymbol{B}, \tag{5}$$

$$T = \frac{p}{\rho}, \tag{6}$$

$$\frac{\partial p}{\partial t} = \mu(\frac{2}{3}(\nabla \cdot \boldsymbol{v})\vec{\boldsymbol{I}} - \nabla \boldsymbol{v} - {}^{t}(\nabla \boldsymbol{v})), \tag{7}$$

where ρ is the mass density, v is the fluid velocity, $\boldsymbol{B}$ is the magnetic field, and p is the plasma pressure. For simplicity, the conductivity κ, the viscosity μ, and the resistivity η are assumed to be uniform constant throughout the whole region. The ratio of specific heats γ is 5/3. The strength of typical magnetic field B_0=0.2 T, and the initial mass density $\rho_0 = 5.0 \times 10^{19}$ m^{-3}, are used for a normalization, respectively. Under the normalization, the velocity and the time are normalized by the Alfvén velocity v_A=620 km/s and the Alfvén transit time τ_A=0.81 μsec, respectively. The grid numbers are chosen to be (N_r, N_θ, N_z) = (39, 64, 40) in the gun region and (N_r, N_θ, N_z) = (69, 64, 121) in the confinement region. As shown in Fig. 4, we divide the simulation region in which the governing equations are solved into two-cylinders with a central conductor inserted along the symmetry axis. One is a gun region ($0.175 \le r \le 0.65$ and $0 \le z \le 0.5$) corresponding to the MCPG region. The other is a confinement region ($0.15 \le r \le 1.0$ and $0.5 \le z \le 2.0$). Bias magnetic flux penetrates electrodes at the inner and outer boundaries of the MCPG region. The radial cross electric field $\boldsymbol{E}_{inj}$ is always applied to the gap between gun electrodes. It is assumed in the simulation that the mass density is spatially and temporally constant and no slip wall condition $v = 0$ at all boundaries. The initial MHD equilibrium configuration for the simulation is given by an axisymmetric force-free equilibrium $\nabla \times \boldsymbol{B} = \lambda \boldsymbol{B}$ which can be obtained by numerically solving a Grad-Shafranov equation under the boundary conditions. Here the force-free parameter λ at the magnetic axis is set as $\lambda_{axis} = 5.0$, $I_{tf} = 0$, and the corresponding safety factor q at the magnetic axis q_{axis}= 0.7.

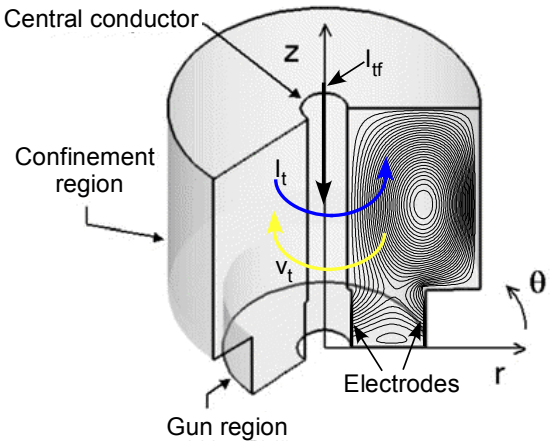

FIG. 4. Schematic view of the simulation region in cylindrical coordinate (r, θ, z).

Figure 5 shows the time evolutions of the toroidal current I_t, the toroidal magnetic flux Ψ_t, the poloidal magnetic flux Ψ_p, and the magnetic energy W_{mag} for each toroidal mode n. We can see in Fig. 5(a) that I_t is successfully sustained against the resistive decay, and I_t, Ψ_t, Ψ_p, and W_{mag} have periodic oscillations after about $t = 800\tau_A$. The oscillations of I_t and Ψ_p are correlated very well. It is also noted that the oscillations of Ψ_p are out of phase with those of Ψ_t, which means that the flux conversion from Ψ_t to Ψ_p occurs during the sustainment. The plasma with oscillating n-mode structures (the n=1 mode has the largest amplitude) rotates in the toroidal direction with frequency f =16 kHz. This plasma rotation due to $\boldsymbol{E} \times \boldsymbol{B}$ drift is in the opposite direction to I_t. This result from magnetic measurements is in agreement with observations in the HIST operated by the spheromak mode (I_{tf}=0) [4].

Figure 6 shows vector plots of B_p and the poloidal flow velocity v_p, and contours of B_t and the toroidal flow velocity v_t. The plasma is ejected from the gun region toward the confinement region. After then, we can seen that the plasma, which is propagating to the confinement region, deforms helically around the central conductor at t=1166τ_A. As the result, the magnetic reconnection event occurs at the X-point near the gun muzzle, and then the toroidal flow ($v_t \approx 37$ km/s) is enhanced around there in the opposite direction to I_t, but in the same direction as the $\boldsymbol{E}\times\boldsymbol{B}$ plasma rotation. This result is consistent with the flow observation in the HIT-II [8], and NSTX [6] experiments. This magnetic reconnection event results in the generation of the closed poloidal field lines like a plasmoid or a vortex at t = 1202τ_A, as shown in Fig. 6. It can be also seen at t = 1224τ_A that the magnetic configuration takes a partially relaxed state, whereas the strong toroidal flow (yellow) remains at the inboard and the toroidal flow (blue) is intensively induced in the opposite direction at the outboard. After then the new plasma are ejected from the injector and this process is repeated with a time interval of ~200τ_A.

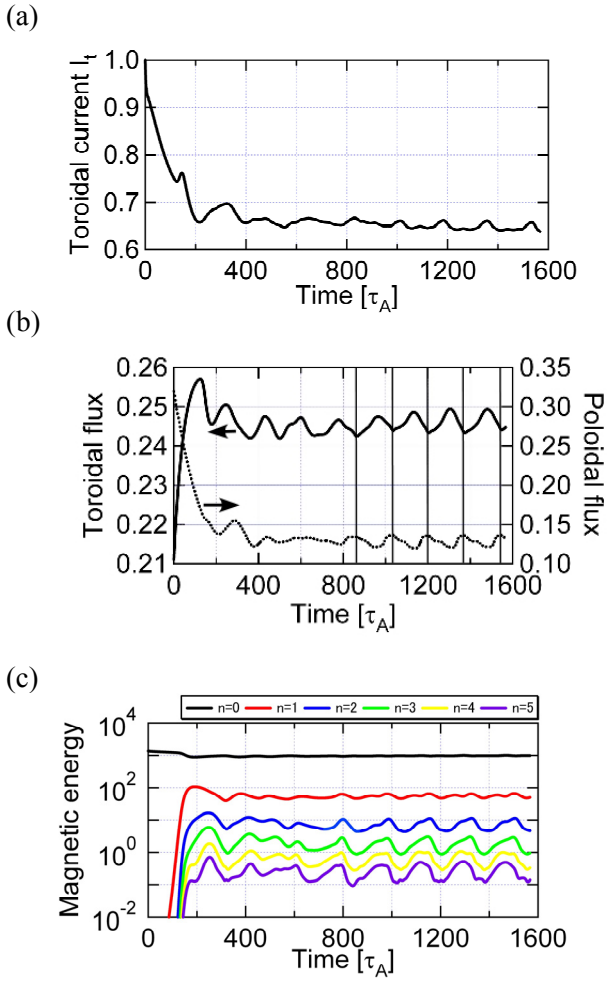

FIG. 5. Time evolutions of the toroidal current (a), the magnetic flux (b), and the magnetic energy for each toroidal Fourier mode n (c).

5. Flow measurements in the formation of F-ST

As for the F-ST, when the TF coil current I_{tf} is decreased and its direction is reversed, the N-ST plasma becomes unstable due to the violation of the Kruskal-Shafranov stability condition (q=1) and then relaxes to the F-ST relaxed state through the RFP-like relaxed state as shown in Fig. 7. It is noted that the RFP plasma formed transiently has an axisymmetric configuration (B_r~0). During the transition process between these configurations, not only the toroidal field (poloidal current) but also the poloidal field (toroidal current) reverses polarity spontaneously. The existence of the force-free flipped relaxed state is predicted based on the Taylor relaxation theory modified in the helicity-driven system. The self-reversal of the magnetic fields is attributed to the non-linear growth of the n=1 kink instability of the central open flux. When the TF is triggered to decrease in the current ramp-up phase, the phase of the n = 1 mode starts to rotate in the opposite direction of I_t (Fig.7 (b)). Thereafter, when the n=1 mode starts to grow at t=0.54 ms (Fig.7 (c)), the direction of the rotation appears to be slightly reversed. At the same time, the poloidal fields measured at the boundary surfaces start to reverse the polarity from the bottom of the FC.

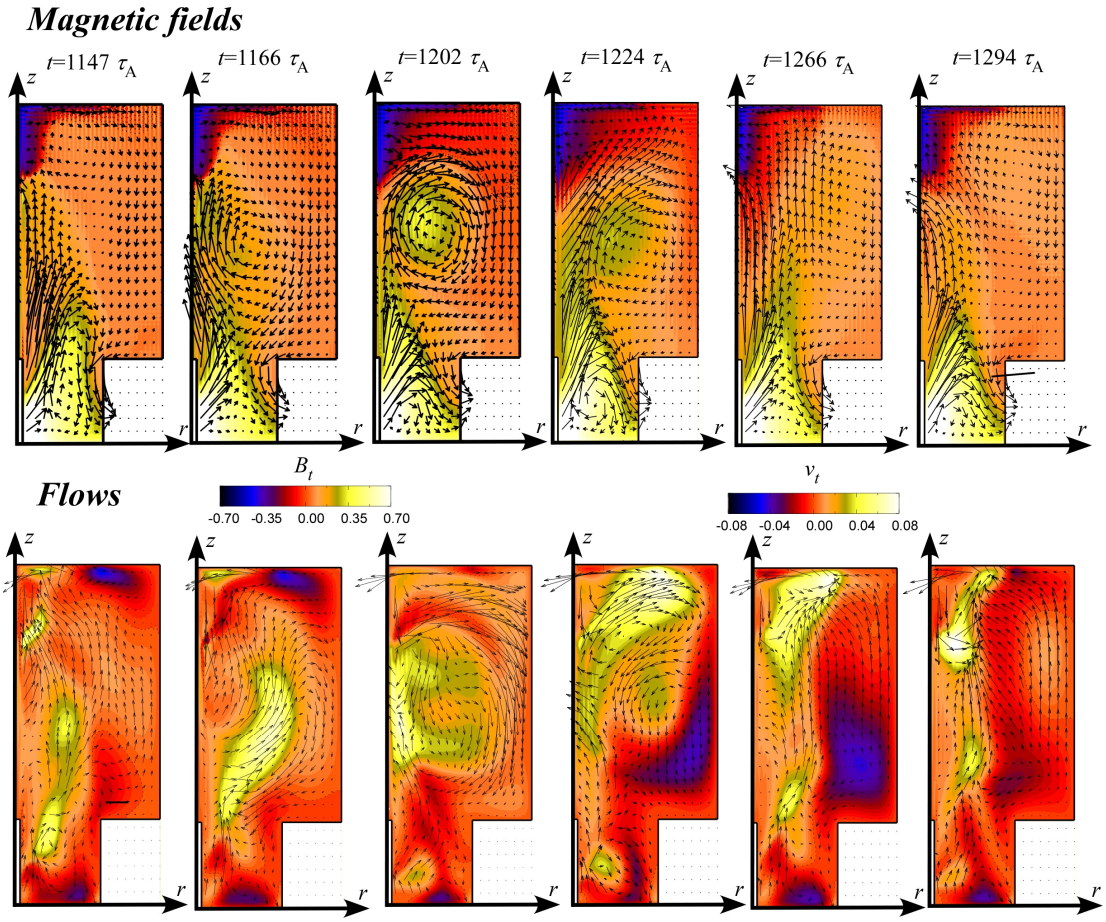

FIG. 6. Vector plots of poloidal magnetic field B_p and contours of toroidal field B_t on the poloidal cross sections $\theta = \pi/2$ rad at $t = 1147\ \tau_A$,$t = 1166\ \tau_A$, $t = 1202\ \tau_A$, $t = 1224\ \tau_A$, $t = 1266\ \tau_A$, and $t = 1294\ \tau_A$. The color on B_t varies from black, blue, red, yellow to white as the magnetic field increases. Vector plots of poloidal flow velocity v_p and contours of toroidal flow velocity v_t on the poloidal cross sections $\theta = \pi/2$ rad at each time. The color on v_t varies from black, blue, red, yellow to white as the flow velocity increases. The color of yellow on the flow contours indicates the opposite direction of the toroidal current and the same direction of $\boldsymbol{E}\times\boldsymbol{B}$.

The Mach probe measurement exhibits that the flow velocity is strongly fluctuated and abruptly increased up to >50 km/s during the current reversal (relaxation) phase as shown in Fig. 8. This enhancement of ion flow velocity is fairly correlated to a bump observed on the electron density signal. The IDS measurement indicates the ion heating from ~10 eV to ~40 eV during the sustainment of the F-ST plasma as shown in Fig. 9. The ion heating is oscillated with correlating closely with the n=1 magnetic fluctuations observed at the outer boundary which is responsible for the sustainment of the F-ST. The ion flow tends to reverse the direction correspondingly as the direction of I_t reverses. 3D MHD numerical simulations studies predict that a large kinking behavior of the open flux around the central conductor and the following magnetic reconnection between open and closed field lines play an important role in the generation of the strong ion flow during the self-reversal process. The experimental observation of the strong driven flow is consistent with the simulation result.

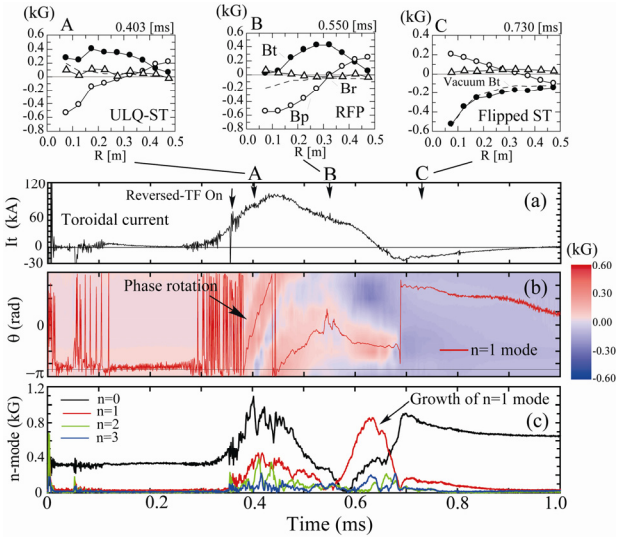

FIG. 7. Time evolution of I_t (a), phase of n=1 mode (I_t direction is -θ) (b) and amplitude of n-modes (c). Radial profile of magnetic fields (A: ULQ-ST, B: RFP, C: F-ST).

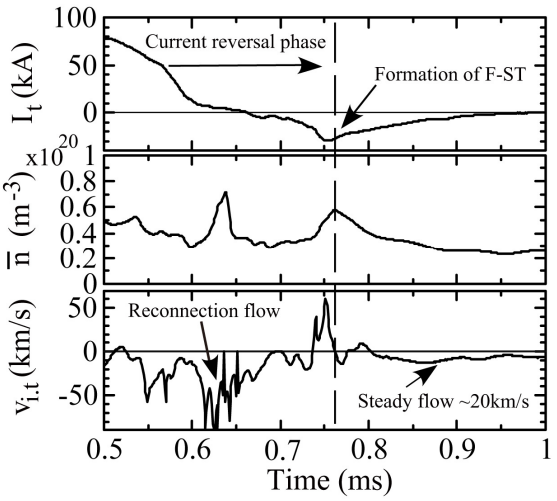

FIG. 8. Time evolution of the toroidal current, averaged electron density and toroidal flow $v_{i,t}$ measured at R=0.25 m during the self-reversal process of currents.

6. Summary

We have for the first time measured the plasma flow by using IDS and Mach probes in order to investigate the CHI current drive of ULQ-ST and the formation and sustainment of the F-ST plasmas. The results are consistent with the model of "repetitive plasmoid ejection and coalescence" proposed for CHI current drive. The current drive mechanisms are supported by the 3D MHD numerical simulation. The acceleration of ion flow has been observed during the formation of the F-ST. The current self-reversal process involves the non-linear development of the *n*=1 kink mode and the following reconnection flow. Ion is anomalously heated by magnetic fluctuations with large amplitude during the sustainment of the F-ST. It is necessary to show more detail comparison between simulation and experimental results.

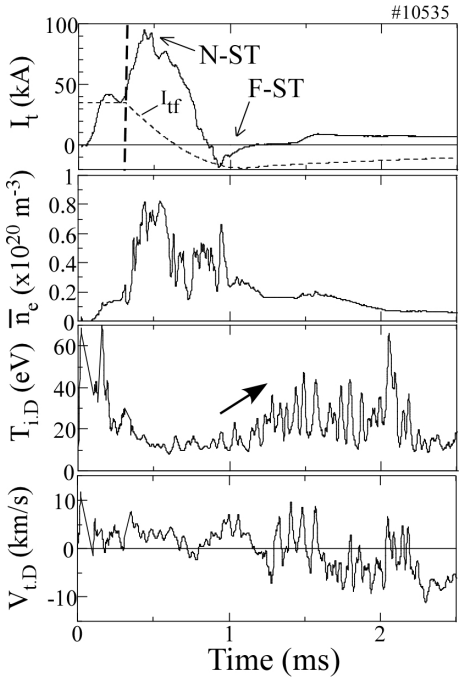

FIG. 9. Time evolution of the toroidal current, averaged electron density, Doppler ion temperature $T_{i,D}$ and toroidal flow speed v_{iD} measured by IDS during the formation and sustainment of the F-ST plasmas.

References

[1] DUEK, R.C., et al., Plasma Phys. Controlled Fusion **39** (1997) 715.
[2] NAGATA, M., et al., Phys. Rev. Lett. **71** (1993) 4342.
[3] McLEAN, H.S., et al., Phys. Rev. Lett. **88** (2002) 125004.
[4] NAGATA, M., et al., Phys. Plasmas **10** (2003) 2932.
[5] REDD, A.J., et al., Phys. Plasmas **14** (2007) 112511.
[6] NAGATA, M., et al., J. Plasma and Fusion Research **2** (2007) 0035.
[7] NAGATA, M., et al., Phys. Rev. Lett. **90** (2003) 225001.
[8] JARBOE, T.R., et al., Nucl. Fusion **41** (2001) 679.
[9] KAGEI, Y., et al., Journal of Plasma and Fusion Research **79** (2003) 217.
[10] KAGEI, Y., et al., Plasma Phys. Control. Fusion **45** (2003) L17.
[11] GU. P., et al., Rev. of Sci. Instrum. **75** (2004) 1337.